

# Semi-Numerical Derivation of the Opening Shock Factor and Inflation Time for Slider-Reefed Parafoils<sup>##</sup>

Jean Potvin<sup>o</sup> and Benjamin Hurst<sup>i</sup>  
Department of Physics, Saint Louis University, St. Louis, MO 63103

Gary Peek<sup>Ⓜ</sup>  
Industrologic, Inc. St. Charles MO, 63301

## Abstract

This paper presents a derivation of the opening shock factor ( $C_k$ ) and inflation duration ( $t_{fill}$ ) that characterize the inflation of slider-reefed parafoils. The results apply to large-mass ratio systems, such as personnel parachutes, that inflate along a downward vertical trajectory and experience maximum drag ( $F_{max}$ ) during slider-descent. The derivation of  $C_k$  is based on a formulas derived from the well-validated inflation computer model discussed in another paper presented at this conference (see paper 2007-2501). The formula for  $t_{fill}$  is obtained by merging this result with a general expression for  $C_k$ , obtained from the Momentum-Impulse theorem in which the inflation time is a crucial input. These derivations are followed by an altitude-scaling study of the maximum deceleration (and force) sustained by the system. The importance of the duration and characteristics of the “slider-up” phase in determining overall inflation performance is also examined.

## Nomenclature

$a(t)$  = Instant value of the parachute-payload acceleration/deceleration  
 $a_{max}$  = Maximum deceleration sustained during the slider descent phase  
 $C_D(t)$  = Instant drag coefficient of the parafoil  
 $C_k$  = Opening shock factor  
 $D_0$  = Nominal diameter  
 $F_{max}$  = Maximum drag force sustained during inflation  
 $F_D^{sliderup}$  = parachute drag during the slider-up phase  
 $g$  = Acceleration of gravity constant  
 $I_F^{if}$  = Drag integral  
 $K$  = Canopy spreading rate constant  
 $L_{chord}$  = Parafoil wing chord  
 $L_{span}$  = Parafoil wing span  
 $L_{sliderspan}$  = Slider span  
 $L_{sliderchord}$  = Slider chord  
 $L_{susplines}$  = Average suspension line length  
 $m$  = Mass of the parachute-payload system  
 $m_{canopy}$  = Canopy fabric mass (without suspension lines)  
 $n_{fill}$  = Non-dimensional inflation (or “filling”) time  
 $R_m$  = Inverse mass ratio  
 $R_p$  = Slider-descent scaling factor

<sup>o</sup> Professor, Department of Physics, 3450 Lindell Blvd, St. Louis, MO 63103; member AIAA

<sup>i</sup> Student, Department of Physics, 3450 Lindell Blvd, St. Louis, MO 63103

<sup>Ⓜ</sup> Consultant, 3201 Highgate Lane, St. Charles, MO 63301

<sup>##</sup> Presented at the 19<sup>th</sup> AIAA Aerodynamic Decelerator Systems Technology Conference, Williamsburg, VA, 21-24 May 2007. **With corrections (06/05/2007).**

$S(t)$  = Instant parafoil opened surface area  
 $S_0$  = Canopy nominal surface area  
 $(SC_D)_{nochute}$  = Steady-state fall rate of the payload prior to parachute deployment  
 $(SC_D)_{sd}$  = Steady-state fall rate (i.e. with fully opened canopy; no gliding)  
 $t$  = Time  
 $t_{fill}$  = Duration of the entire opening sequence, including the slider-up and slider-descent phase  
 $t_{max}$  = Time of maximum deceleration during slider descent  
 $V(t)$  = Instant value of the parachute-payload rate of descent  
 $V_{descent}$  = Parafoil steady-state descent speed in a “no-glide”, flat-plate configuration  
 $V_{ls} = V_{stretch}$  = Fall rate of the parachute-payload system at the moment of suspension line stretch  
 $V_f$  = Descent rate of the system at the end of the inflation process  
 $V_0$  = Fall rate of the system at the end of the slider-up phase (i.e. just prior to slider-descent)  
 $W$  = Total weight (including parachute fabric and payload weight)  
 $V_{ff}$  = Fall rate of the payload, without the parachute (=  $V_{stretch}$  in this paper)  
  
 $\Delta t_{sliderup}$  = Duration of the slider-up phase  
 $\Gamma$  = Momentum per mass change (defined in equation (15))  
 $\rho$  = air density at deployment altitude  
 $\Sigma(t)$  = Instant drag area of the parafoil ( $\equiv C_D(t) S(t)$ )  
 $\Sigma_0$  = Drag area of the canopy during slider-up (constant drag-area scenario)  
 $\Sigma_{slider}^{extra}$  = Extra slider drag area (generated by PCS pilot chute, slider dome geometry, etc.)  
 $\Sigma_{slider}$  = Slider drag area (from fabric within grommeted frame)  
 $\langle \Delta(t) \rangle$  = Average value of the dynamical factor of the canopy spreading rate constant [1]

## I. Introduction

A new dynamical model of slider-reefed parafoil inflation was defined and discussed in a paper also presented at this conference [1]. The model includes a detailed picture of the inflation processes at play during the all-important slider-up phase, as well as a model for the slider-descent phase that was previously explored in references [2, 3]. An example of the kind of good match with experimental data that was obtained is shown in figure 1 below. The resulting inflation simulations are specific enough in terms of the inflation processes and design characteristics to allow a systematic study of the various factors and canopy components that affect slider-reefed parafoil inflation in general. For example, the model shows how the randomness associated with surging motions and fabric flapping come into play and influence the duration of the early parts of the inflation process. The high level of design details shows also how several factors can compete in ways that either enhance, or cancel out desired changes in inflation performance.

This paper explores some of the general inflation phenomenology that arises from this model, via the derivation of formulas describing two of the most important inflation performance parameters sought after by engineers, namely the opening shock factor ( $C_k$ ) and the inflation time ( $t_{fill}$ ). Such “derivations” will be based on the generation of hundreds of computer simulations of the model, and on the fitting of this numerical data to simple functions. These derivations shall show how drastically different the opening force experienced during the slider-descent phase can become when the randomness associated with the inflation rates during the slider-up phase is taken into account. The main result of this paper is that there is not one, but rather *several* scaling laws that are to guide the dependence of maximum drag and overall inflation duration on canopy and slider characteristics. Such behavior alone explains why parafoil inflation characteristics do change so drastically even on a jump-to-jump basis.

## II. Derivation of the Opening Shock Factor

### A. General definition

The opening shock factor  $C_k$  is a non-dimensional ratio that corresponds to the maximum drag force  $F_{max}$  generated by an inflating parachute, herein calculated by the model of reference [1]. It is defined as follows [4 – 6]:

$$C_k \equiv \frac{F_{max}}{(SC_D)_{sd} \left( \frac{1}{2} \rho V_{stretch}^2 \right)} \quad (1)$$

This ratio is expressed in terms of the dynamic pressure sustained by the parachute–payload system at the beginning of the inflation process, most typically at the moment of the full stretching of the suspension lines, and also in terms of the parafoil’s steady-descent drag area  $(SC_D)_{sd}$ . Here  $(SC_D)_{sd}$  corresponds to a canopy descending in “flat-plate”, non-gliding mode and is calculated as  $(SC_D)_{sd} = 1.0 L_{span} L_{chord}$ . The symbol  $\rho$  corresponds to the value of the atmospheric density at deployment altitude, and  $m$  to the total mass of the parachute-payload system. Ewing, Bixby, Schilling, Knacke and others [4, 5], and then Wolf [6], have shown that graphing  $C_k$  in terms of the “inverse” mass ratio  $R_m \equiv \rho (SC_D)_{sd}^{3/2}/m$  displays the inflation data of hemispherical parachutes into two well-defined bands. Reference [7], on the other hand, shows how to plot these two bands on the same  $C_k$ - $R_m$  graph by involving the explicit use of the non-dimensional filling time  $n_{fill} (\equiv V_{stretch} t_{fill}/D_0)$ . (This reference also shows how to graph the data of *any* parachute canopy shape and reefing design). Here  $t_{fill}$  is the duration of the entire inflation sequence, and  $D_0$  the nominal canopy diameter calculated from the total canopy surface area  $S_0$  as  $D_0 = (4S_0/\pi)^{1/2}$  [4]. For parafoils,  $S_0$  is given by the product of the chord and span [8]. Such dependence of  $C_k$  on the mass ratio makes sense since the latter is an estimate of the air mass that decelerates (or accelerates) along with the parachute system during inflation. As such, it is an indicator of the type of acceleration/deceleration profile that is being sustained by the parachute-payload system, and ultimately, of the type of parachute wakes that is emerging during canopy expansion [9]. So far  $C_k$  and  $F_{max}$  have been mostly extracted from experimental data, with the exception of Doherr’s study of the Pflanz-Ludtke model [10].

## B. Numerical model of slider-descent

The first ingredient of the semi-numerical derivation of  $F_{max}$  and  $C_k$  shall be based on the simulation of the slider-descent phase of parafoil inflation, which is the phase that precedes the so-called “slider-up” phase [1 - 3]. For most applications, **slider-descent is the phase during which the maximum drag force  $F_{max}$  is being generated by the opening canopy**. It can be argued on dimensional grounds that the simplest relationship linking instant drag area  $S(t)C_D(t)$  to the fall rate  $V(t)$  during this phase is given by:

$$\frac{d^2(C_D(t)S(t))}{dt^2} = KV(t)^2 \quad (2)$$

The constant  $K$  is a non-dimensional input parameter, named *canopy/wing spreading rate* constant. By comparing with empirical data, it is argued in [1] and [11] that the spreading rate constant can be estimated from the following expression:

$$K \sim \Psi \frac{L_{span} L_{chord}}{(\rho L_{chord}^3 + m_{canopy}) L_{susplines}} \rho (\Sigma_{slider} + \Sigma_{slider}^{extra}) \left( \frac{L_{span}}{L_{sliderspan} + \sqrt{\Sigma_{slider}^{extra}}} \right) \langle \Delta \rangle \quad (3)$$

Here  $\Psi \sim 1/5$  and  $\langle \Delta \rangle \sim (1 \pm 0.5)$ , the latter being a factor simulating the jump-to-jump variations that are so prevalent in parafoil inflation. Besides the usual canopy wing chord ( $L_{chord}$ ) and span ( $L_{span}$ ) lengths, this equation depends explicitly on the mass of the canopy itself ( $m_{canopy}$ ), the average length of the suspension lines ( $L_{susplines}$ ), the span of the slider ( $L_{sliderspan}$ ), the slider drag area ( $\Sigma_{slider} = C_D S_{slider}$ ) and, in the case of a *pilot-chute-controlled slider* [11, 12], the drag area of the pilot chute  $\Sigma_{slider}^{extra}$ . Note that there is no dependence on wing inlet area; such dependence appears only explicitly in the slider-up phase as further discussed in [1, 11]. Note finally that this result applies mostly to “**tuned**”/balanced canopies, i.e. canopies that have their steering line rigged in such a way to minimize parafoil-generated lift (and therefore surging) during inflation. This slider-descent model has done a good job at reproducing about 80% of the drops/jumps performed on the tuned canopies under consideration, as shown with the example of figure 1; more details and curves are provided in [1, 11]. Finally, as noted in [1] again, equation (3) should be expected to become quite inaccurate when the friction between the slider grommets and suspension line becomes very high, such as with old, worn, abraded lines. Interestingly, the value of grommet friction does not appear explicitly in (3); it is however a crucial factor in determining the duration of the slider-up phase [1].

The numerical computation of (2) and (3), together with that of the parachute-payload’s Newtonian equation of motion applied to vertical trajectories during slider-descent produce the maximum deceleration data ( $a_{max}/g$ ) and time of maximum deceleration data ( $t_{max}g/V_0$ ) shown in figure 2 (such data was generated from over 2000 simulations [2]). Note that  $t_{max}$  is measured with respect to the beginning of the slider-descent phase, and as such will never be equal to  $t_{fill}$  (i.e. duration of the combined slider-up and slider-descent phases). Similarly,  $V_0$  is the fall rate of the system at the

beginning of slider-descent, and will in general be different from the fall rate  $V_{ls}$  ( $\equiv V_{stretch}$ ) at the time of line stretch. Finally,  $g$  is the constant of gravitational acceleration.

The data of figure 2 shows an interesting exponential dependence when graphed in terms of the non-dimensional ratio  $R_p$  [2]:

$$R_p = \frac{\rho K V_0^6}{2Wg^2} \quad (4)$$

Indeed, curve-fitting this data to an exponential form yields [2]:

$$\frac{a_{max}}{g} = 0.360 R_p^{0.332} \quad (5)$$

$$\frac{t_{max} g}{V_0} = 1.532 R_p^{-0.354} \quad (6)$$

Here  $W$  is the total weight of the parachute-payload system. The value of  $a_{max}$  is related to that of  $F_{max}$  via the definition  $a_{max} \equiv (F_{max} - W)/m$  (vertical trajectory). The opening shock factor  $C_k$  is then obtained by combining (4) and (5) with (1), along with using the mass ratio  $R_m$  as defined in Section II.A:

$$C_k = \left[ \frac{0.57 K^{1/3}}{(R_m)^{2/3}} + \frac{2W}{\rho(SC_D)_{fullopen} V_0^2} \right] \left( \frac{V_0}{V_{ls}} \right)^2 \quad (7)$$

Note that this result was derived by assuming  $0.332 \sim 1/3$ . Remember again that the value of the canopy spreading constant  $K$  is computed via equation (3).

This result can be simplified further if one uses the “flat-plate”, no-glide steady-descent speed defined by  $V_{descent} = 2W/\rho L_{span} L_{chord}$ :

$$C_k = \frac{0.57 K^{1/3}}{R_m^{2/3}} \left( \frac{V_0}{V_{stretch}} \right)^2 + \left( \frac{V_{descent}}{V_{stretch}} \right)^2 \approx \frac{0.57 K^{1/3}}{R_m^{2/3}} \left( \frac{V_0}{V_{stretch}} \right)^2 \quad (8)$$

The last equality would apply (at least) to personnel parachuting applications, where typically  $V_{descent} < 30 \text{ ft/sec}$  [9],  $V_{stretch} \sim 150 - 180 \text{ ft/sec}$  and therefore  $V_{descent} \ll V_{stretch}$ . This approximation would not work for BASE jumping, where  $V_{descent} \sim V_{stretch}$ .

Besides its simplicity, equation (8) is remarkable for many other reasons, first among which, its dependence on the canopy spreading rate constant as  $K^{1/3}$ , and on the mass ratio as  $R_m^{-2/3}$ . Noted many years ago in [2], such a weak dependence on  $K$  means that its accurate knowledge is not necessary for the estimation of  $a_{max}$ ,  $F_{max}$  or  $C_k$ . In fact, estimating  $K$  from (3) while using  $\Delta = 1$  appears to be good enough. On the other hand, having  $C_k$  being proportional to  $K^{1/3}/R_m^{2/3}$  is consistent with the intuitive notion that the faster the rate of canopy spreading, and/or the smaller the mass ratio, the higher the opening forces. Finally, equation (8) explains why graphing  $C_k$  vs.  $R_m$  never follows a single curve, but rather an infinite number of curves, with each curve being defined by factors related to specific design features [4 – 6]. In fact, reference [7] shows quite generally that  $C_k$  is proportional to  $1/(t_{fill} R_m)$  and to other factors related to canopy size and trajectory type; this relation is shown in equation (13) below. The fact that  $C_k \sim R_m^{-2/3}$  in equation (8), in contrast to  $C_k \sim R_m^{-3/3}$  as shown in reference [7], has to do with the explicit absence of  $t_{fill}$  and other parameters in (8). On the other hand, the comparison suggests that  $t_{fill}$  and other parameters depend on the mass ratio  $R_m$  only weakly.

Most importantly, equation (8) indicates the importance of the contrast between  $V_0$  and  $V_{stretch}$  in determining how high  $F_{max}$  and  $C_k$  shall be. For example, the more deceleration during the slider-up phase, the smaller the  $V_0$  and thereby the smaller the  $F_{max}$  and  $C_k$ . Looking at how equation (8) depends on the input parameters  $R_m$ ,  $K$  and  $(V(0)/V_{stretch})$  shows that  $V(0)/V_{stretch}$  is by far the most important. Therefore, drastically different durations of the slider-up phase shall yield drastically different values of  $V_0$ , and thereby substantially different values of  $F_{max}$  and  $C_k$ . Moreover, such a relationship implies that  $F_{max}$  and  $C_k$  shall also vary on a jump-to-jump basis whenever the ratio  $V(0)/V_{stretch}$  changes on a jump-to-jump basis, for example as a result of the randomness associated with the durations

of the slider-up phase [1]. These results make clear the important fact that the inflation characteristics during slider-descent will be strongly dependent on what happens during the slider-up phase.

Note again that equation (8) is only valid when  $F_{max}$  is being experienced during the slider-descent phase, an event that happens to most, but not all parafoil openings [1]. In cases where the latter event is occurring, it is clear that  $F_{max}$  and  $C_k$  will exhibit strikingly different scaling laws, i.e. laws that would be independent of  $K$  as well as of most of the canopy construction characteristics that are featured in the fully-opened configuration.

It should be added that using equation (8) along with an *a priori* known  $C_k$  gives the means to predict at least an average value of  $V_0$  – an opening performance variable that is quite difficult to measure experimentally. For example, a canopy characterized by  $K \sim 0.1$ , such as the skydiving canopies discussed in references [1] and [11], yields  $R_m \sim 1$ ; together with  $C_k \sim 0.1$  [7] and  $V_{stretch} \sim 176 \text{ ft/sec}$  one would have  $V_0 \sim 108 \text{ ft/sec}$ .

### C. $V_0$ -Scaling

By definition  $V_0$  characterizes the fall speed at the end of the slider-up phase, i.e. just prior to slider-descent. The extensive database analyzed in [1, 11] shows that slider-reefed parafoils inflate in different “modes”, as a result of the many ways the air can enter or exit a parafoil’s center and outboard cells, either at the moment of line-stretch or during the rest of the slider-up phase. Therefore it should not be surprising to find that inlet dynamics is a major determinant of slider-up duration ( $\Delta t_{sliderup}$ ) and of  $V_0$ . This is shown explicitly in figure 3 below, where the ratio  $(V_{stretch} - V_0)/V_{stretch}$  is plotted versus the ratio  $g\Delta t_{sliderup}/V_{stretch}$ , a non-dimensional measure of slider-up phase duration. The data on this graph was obtained by running several simulations while changing the deployment altitude, effective inlet dimensions, payload mass and value of  $V_{stretch}$ . The detailed analysis discussed in [1, 11] points to at least three different modes of slider-up inflation evolution which are shown in figure 1, 4 and 5:

- **Short slider-up phase**
- **Constant-drag force**
- **Constant-drag area**

Each one of those modes can be described as follows:

#### - *Very short slider-up phase (figure 5)*

This type of evolution is caused by many factors, among which:

- Large initial “gulp” of air into the cells, a scenario that could occur when *all* of the wing’s inlets are simultaneously wide-open after bag strip, to allow an unusually large amount of air to enter each cell
- Line dumps, generated because of faulty rigging (usually), or when the suspension lines are deployed at the same time the canopy is pulled out of the bag (usually the former precedes the latter);
- Premature slider motion – a case that arises when bag strip is violent enough to displace the slider (downward), and allow further opening of the cell inlets and premature inflation of the cell located beyond the slider span (i.e. cells at the wing tips and at  $\frac{1}{4}$  and  $\frac{3}{4}$  span);
- “Bottom skin opening” – a scenario enabled when the air stream quickly pushes the slider downwards and spreads the underside of the canopy *before* any cell inflation has taken place

In all these cases the result is the same, namely that of  $V_0$  being pretty close to the fall rate  $V_{ff}$  of the parachute-payload system just prior to parachute deployment. In the case of a long pre-deployment freefall one could consider the following approximation:

$$V_0 \approx V_{ff} = \sqrt{\frac{2W}{\rho(SC_D)_{nochute}}} \quad (9)$$

with  $(SC_D)_{nochute}$  corresponding to the drag area of the payload container during a steady-state fall prior to parachute opening.

#### - *Constant-drag force during the slider-up phase (figure 1)*

This case characterizes the inflation evolution of a very large number of parafoil designs from the mid-1990’s onward. It is seen rather frequently, even on a jump-to-jump basis. These newer parafoils feature smaller inlet sizes

and larger sliders than their brethren of the 1980's. A possible consequence of these characteristics is that the decrease in the squared parachute-payload fall rate  $V(t)^2$  is matched almost exactly by a slow increase in drag area, in a manner that results in a near-constant drag force evolution of the type shown in figure 1. In this case the motion of the system is described by simple constant-acceleration kinematics:

$$V_0 \approx \left| a \Delta t_{sliderup} - V_{ff} \right| = \left| \frac{F_D^{sliderup}}{m} \Delta t_{sliderup} - V_{ff} \right| \quad (10)$$

$$= \left| \frac{\rho \left[ S(t) C_D(t) V(t)^2 \right]}{2m} \Delta t_{sliderup} - V_{ff} \right| \sim \left| \frac{\rho [const]}{2m} \Delta t_{sliderup} - V_{ff} \right|$$

The value of the parameter  $\Delta t_{sliderup}$  is of the order of 1 -to- 2 seconds on personnel parachute systems;  $F_D^{sliderup}$  is the constant drag force generated by the inflating parachute during that phase, as a result of the product  $S(t)C_D(t)V(t)^2$  nearly being constant. Note that it is not uncommon to see  $F_D^{sliderup} \sim 2W$  empirically (figure 1 shows one such case). Considering this particular trend as an average, one has

$$V_0 \approx \left| a \Delta t_{sliderup} - V_{ff} \right| = \left| \left( \frac{F_D^{sliderup} - W}{m} \right) \Delta t_{sliderup} - V_{ff} \right| \quad (11)$$

$$\sim \left| \left( \frac{2W - W}{m} \right) \Delta t_{sliderup} - V_{ff} \right|$$

Equation (11) should be seen only as a gross average, with possibly large deviations as suggested in the simulations of figure 3.

- *Constant-drag area during the slider-up phase (figure 4)*

References [2, 3] used the assumption of  $S(t)C_D(t) \sim const$  on the basis of simplicity rather than realism. Such a mode has been seen, but only rarely – see figure 4 for example. In this case the equation of motion of the parachute-payload system can be readily integrated, to yield [2]:

$$V_0 = \left| V_T \left( \frac{Ae^{\frac{-V_T \Delta t_{sliderup}}{D}} + 1}{Ae^{\frac{-V_T \Delta t_{sliderup}}{D}} - 1} \right) \right| \quad (12)$$

where

$$m = W/g$$

$$D = m/(\rho \Sigma_0)$$

$$A = (-V_{ff} + V_T)/(-V_{ff} - V_T)$$

$$V_T^2 = 2W/(\rho \Sigma_0)$$

$$V_{ff} > 0 \text{ and } V_T > 0.$$

The parameter  $V_T$  corresponds to the terminal fall speed of the payload when suspended a fixed drag area  $\Sigma_0$  equal to the parachute's during the slider-up stage.

To conclude this section: given the importance of the initial speed  $V_0$  in equation (7), it is clear that the scaling behavior of  $C_k$  will depend strongly on the inflation mode characterizing the slider-up phase. **Thus, it should not be surprising to find that, with respect to changes of a given construction- or drop-input parameter, the same parachute system could exhibit more than just one type of scaling behavior.** The scaling properties of (7) shall be discussed further in Section IV.

### III. Derivation of the Inflation Time

The total inflation time  $t_{fill}$  can be obtained by merging equation (5) into a general definition of the opening shock factor obtained from the Momentum-Impulse Theorem [7]:

$$C_k = \frac{2}{I_F^{if} n_{fill} R_m} \frac{\sqrt{(SC_D)_{sd}}}{D_0} \Gamma \quad (13)$$

where

$$I_F^{if} = \int_i^f \frac{|F_D(t)| dt}{F_{max} t_{fill}} \quad (14)$$

$$\Gamma \equiv 1 - \frac{V_f}{V_{stretch}} + n_{fill} \frac{gD_0}{(V_{stretch})^2} \quad (15)$$

Here  $V_f$  is the descent rate of the system at the end of the inflation process. Once again,  $V_{stretch}$  is the fall rate of the parachute-payload system at line-stretch and  $n_{fill}$  the non-dimensional total inflation time (see Section II.A). Equation (14) represents so-called drag integral, defined as the normalized area under the  $F_D(t)$  -vs-  $t$  curve. As discussed in more details in [7] and [9], one has  $I_F^{if} \sim 1/2 \pm 50\%$  at large- $R_m$ , i.e. for personnel parachute systems. The factor  $\Gamma$  corresponds to the system's net change of momentum per unit mass and per unit speed. Note that the third term in  $\Gamma$  represents the momentum gained by the system due to gravity and (partially) lost through drag (i.e. the so-called "Froude" term). Note finally that as with (7), equation (15) applies only to purely vertical trajectories. The mass ratio dependence of (13) has been discussed in details in reference [7] and also in another paper presented at this conference [9]. At large- $R_m$  and "small"- $D_0$  where  $V_f \ll V_{stretch}$  and  $V_i^2 \gg gD_0$ , it was argued that  $C_k \sim 2/(I_F^{if} n_{fill} R_m)$  in general. This can be compared with equation (7) above, where  $C_k \sim 1/R_m^{2/3}$  when  $F_{max} \gg W$ . The difference between the two is, of course, that the factor  $\Gamma/I_F^{if} n_{fill}$  is being factored-in differently in (7) and is implicitly containing some  $R_m$ -dependence.

Combining (8) and (13) in the regime where  $V_{descent} \ll V_{stretch}$  gives an opportunity to derive an expression for the non-dimensional duration  $n_{fill}$  of the entire inflation process:

$$n_{fill} = \frac{\left(1 - \frac{V_{descent}}{V_{stretch}}\right)}{\left[\frac{I_F^{if} D_0 R_m}{2\sqrt{(SC_D)_{sd}}} \frac{0.57 K^{1/3}}{R_m^{2/3}} \left(\frac{V_0}{V_{stretch}}\right)^2\right] - \frac{gD_0}{V_{stretch}^2}} \quad (16a)$$

$$n_{fill} \sim \frac{\left(1 - \frac{V_{descent}}{V_{stretch}}\right)}{\left[\frac{I_F^{if} D_0 R_m}{2\sqrt{(SC_D)_{sd}}} \frac{0.57 K^{1/3}}{R_m^{2/3}} \left(\frac{V_0}{V_{stretch}}\right)^2\right]} \quad (16b)$$

Note that (16b) applies whenever  $gD_0 \ll V_{stretch}^2$ , including personnel parachute applications involving freefalls and/or jumps from fast aircraft. Once again, the previous discussion on the dependence of  $V_0$  on slider-up inflation modes entails that the total inflation time shall also be closely coupled to the type of inflation mode during the slider-up phase. For skydiving parafoils designed in the 1990's, equation (16) yields  $n_{fill} \sim 20 - 30$  in agreement with the experimental data.

Another and very interesting result emerges when merging equations (6) and (16b) together, an operation that yields a direct comparison between  $t_{fill}$  and  $t_{max}$ , the latter being the time of maximum force/deceleration since the beginning of slider-descent:

$$\frac{t_{fill}}{t_{max}} \approx \left( \frac{1.82}{I_F^{ff}} \right) \left( 1 - \frac{V_{descent}}{V_{stretch}} \right) \frac{V_{stretch}}{V_0} \approx 3.64 \frac{V_{stretch}}{V_0} \quad (17)$$

The last equality results from remembering that (16b) holds because  $V_{descent} \ll V_{stretch}$ , and from assuming  $I_F^{ff} \sim 1/2$ , as with personnel parachute applications [7, 9]. This new result compares the entire duration of parafoil opening (i.e.  $t_{fill}$ ), including both slider-up and slider-descent phases, to the time it takes to achieve maximum force, as measured from the moment the slider begins to move downwards. Obviously, this duration ratio should always be greater than unity, and in fact much greater than unity in those cases where the opening parachute spends most of its time in the slider-up phase. In this case the parachute-payload system decelerates substantially during this phase, leading to  $V_0$  being much smaller than  $V_{stretch}$ . What's more, it should be noted that (17) is independent of the canopy spreading constant  $K$  – a result that arises from the fact that both  $n_{fill}$  and  $t_{max}$  have an explicit dependence on  $K^{1/3}$ . But it should be remembered that the latter is an approximation, as it involves simplifying the exponents of (5) and (6) as  $0.332 \sim 0.354 \sim 1/3$ . The interesting feature here is the dependence on the shape of the  $F_D$ -vs- $t$  curve through the value of the drag integral  $I_F^{ff}$ . As discussed further in reference [9], a  $F_D$ -vs- $t$  curve that is roughly triangular in shape (short slider-up phase) will involve  $I_F^{ff} \sim 0.5$  while a curve with a longer slider-up phase of the type shown in figure 1 will have  $I_F^{ff} \sim 0.4$  and therefore a larger  $t_{fill}/t_{max}$ -ratio. Regardless, one wonders whether (17) is a manifestation of a more fundamental behavior, or is an artifact of the 3-phase model.

Note that (17) yields another way to estimate the hard-to-measure pre-slider-descent speed  $V_0$ . Indeed, it allows using load cell data (to compute  $I_F^{ff}$ ), barograph data (to record  $V_{stretch} \sim V_{freefall}$ ) and video data (to measure  $t_{fill}$ ) to compute the value of  $V_0$  at the beginning of slider-descent. In the inflation-case showcased in figure 2 for example,  $t_{fill} \sim 2.5$  sec. and  $t_{max} \sim 0.5$  sec., thereby yielding  $V_{stretch}/V_0 \sim 1.37$ , or  $V_0 \sim 128$  ft/sec in this case, since  $V_{stretch} \sim 176$  ft/sec [9, 11].

#### IV. Scaling With Respect to Deployment Altitude

References [2] and [3] presented a first-ever derivation of the scaling properties of  $F_{max}$  for those slider-reefed parafoils experiencing  $F_{max}$  during the slider-descent phase. Relevant scaling laws were produced for cases involving changes in overall wing surface area, payload weight or deployment altitude. But this analysis depended on using (5) and (6) together with equation (12) to give  $V_0$  in the case of a constant drag area during slider-up – a scenario that we know today occurs only rarely. The altitude scaling analysis is hereby repeated, using this time the  $V_0$ -expressions that arise from the other two (and more common) inflation modes identified Section II.C.

Reference [2] shows that, in the constant-drag area scenario (i.e. Eq. (12)), the value of  $V_0$  scales with respect to air density as  $V_0 \sim 1/\rho^{1/2}$ . Using this result together with the fact that  $K$  scales as  $K \sim \rho^1$  (Eq. (3)), one gets from (5) the following scaling law for maximum deceleration:  $a_{max} \sim \rho^{1/3} K^{1/3} V_0^2 \sim \rho^{1/3} \rho^{1/3} \rho^{-1} \sim \rho^{-1/3}$ . Given that  $ma_{max} \equiv (F_{max} - W)$ , this result shows a moderate increase of the maximum force by a factor of about  $2^{1/3} = 1.26$  when  $F_{max} \gg W$  and when comparing deployments at sea-level and at 20,000ft MSL. It turns out that this scaling trend also takes place with parafoil openings involving very short slider-up phases (Eq. (9)), as  $V_0 \sim V_{ff} \sim 1/\rho^{1/2}$  as well. A different scaling behavior might be expected, on the other hand, with inflation evolutions involving constant drag during the slider-up phase, a case represented by (11). Given that  $V_0 \approx |g \Delta t_{sliderup} - V_{ff}|$  and that  $\Delta t_{sliderup}$  scales as  $\Delta t_{sliderup} \sim 1/V_{ff}$ , and finally the fact that  $V_{ff}$  scales as  $V_{ff} \sim 1/\rho^{1/2}$  (see Eq. (9)), one obtains a scaling behavior for  $V_0$  that shall depend strongly on how large the term in  $g \Delta t_{sliderup}$  is compared to  $V_{ff}$ . For short slider-up times one has again  $V_0 \sim V_{ff} \sim 1/\rho^{1/2}$ , which once more yields the results derived in [2]. For longer slider-up times, on the other hand, the effect of the  $g \Delta t_{sliderup}$  –term becomes weaker at higher altitude than near the ground, in a manner akin to  $\sim (\rho - 1/\rho)$ . Thus one should expect the value of  $V_0$  to be somewhat more insensitive to the reduction of air density, and expect the force increase to be somewhat less than  $2^{1/3} = 1.26$  (comparing again deployments near sea-level and at 20,000ft MSL). At least as far as altitude-scaling is concerned, the overall results of [2] still apply, except for those cases for which  $g \Delta t_{sliderup}$  is commensurate with  $V_{ff}$ .



## V. Concluding Remarks

Even though the 3-stage model of reference [1] can be always be fully solved with a single numerical simulation, a great deal more can be learned by studying how a large number of computed values for  $F_{max}$ ,  $C_k$ ,  $t_{fill}$  and  $t_{max}$  do scale with respect to changes in deployment altitude, overall wing size, effective inlet dimensions, payload weights, etc. This paper shows that such scaling behavior will be strongly dependent on the specific inflation evolution during the slider-up phase, a fact that is mostly encapsulated into the value of  $V_0$ .

Specifics of the analysis shows that the opening shock factor  $C_k$  indeed decreases with increasing mass ratios, for example with decreasing payload weight at fixed wing size, in qualitative agreement with [4 - 7], and in a manner proportional to  $R_m^{-2/3}$ . The analysis shows also that the ratio of the duration of the slider-descent phase (i.e.  $\sim 2t_{max}$ ) to that of the entire opening sequence (i.e.  $t_{fill}$ ), is proportional to the ratio  $V_0/V_{stretch}$ . Interestingly, the results also suggest how important the actual shape of the drag -versus- time curve influences the value of this duration ratio through the value of the drag integral  $I_F^{df}$ .

The reader should be reminded that the results derived here apply only to tuned canopies used in situations where: 1) the fall trajectory is purely vertical; 2) the steady-descent speeds of the inflated parafoil (in flat-plate, no gliding mode) is much smaller than  $V_{stretch}$ ; 3) the Froude number is small (i.e.  $gD_0 \ll V_{stretch}^2$ ); and finally, 4) the value of  $F_{max}$  occurs during slider-descent. Thus further analysis remains to be performed, especially for those cases where  $F_{max}$  takes place during the slider-up phase instead of the slider-descent phase. Such an analysis shall yield interesting results on its own right, and add new entries to an already full catalog of parafoil inflation scaling laws.

## Acknowledgements

This work was performed with funding from the Natick Soldier Center (Natick, MA) under U.S. Army contract W9124R-05-P-1206. The authors wish to acknowledge the many fruitful discussions with R. Charles, K. Desabrais, C. K. Lee and J. A. Milette, from the Natick Soldier Center.

## References

- [1] Potvin J. and Peek G.; "Three-Stage Model for Slider-Reefed Parafoil Inflation"; paper AIAA-2007-2501; 19<sup>th</sup> AIAA Aerodynamic Decelerator Systems Technology Conference, Williamsburg, VA, 21 - 24 May 2007.
- [2] Potvin, J., Peek, G. and Brocato, B.; "Modeling the Inflation of ram-air Parachutes reefed with Sliders"; *Journal of Aircraft*; **38**, No.5, pp. 818-827, 2001.
- [3] Potvin, J. ; "Altitude- and Weight Scaling Laws for Ram-Air Parachute Inflation" *Journal of Aircraft*, **38**, No. 5, pp. 956-958, 2001.
- [4] T. W. Knacke, "Parachute Recovery Systems Design Manual"; Para Publishing (Santa Barbara, CA 1992).
- [5] Ewing, E. G., Bixby, H. W. and Knacke, T. W.; "Recovery Systems Design guide"; pp. 254 – 257; report AFFL-TR-78-151. Submitted to: Air Force Flight Dynamics Laboratory, AF Wright Aeronautical Laboratories, Wright-Patterson Air Force Base, December 1978. Unpublished.
- [6] Wolf, D., "Opening Shock", AIAA-99-1702, 15<sup>th</sup> CEAS/AIAA Aerodynamic Decelerator Systems Technology Conference, Toulouse, France, 8-11 June 1999.
- [7] Potvin, J.; "Universality Considerations for Graphing Parachute Opening Shock Factor Versus Mass Ratio"; *Journal of Aircraft*; **44**, no. 2, pp. 528 - 538, 2007.
- [8] Lingard, S. J.; *Ram-Air Parachute Design*; AIAA Aerodynamic Decelerator Systems Technology Seminar; May, 1995; 63 pp. Unpublished.
- [9] Potvin J. and Peek G.; "Testing Without Load Cells – Can Opening Shock Be Estimated From Video Only?"; paper AIAA-2007-2551; 19<sup>th</sup> AIAA Aerodynamic Decelerator Systems Technology Conference, Williamsburg, VA, 21 - 24 May 2007.
- [10] Doherr, K., -F; "Extended Parachute Opening Shock Estimation Method"; paper, AIAA-2003-2173; 17<sup>th</sup> AIAA Aerodynamic Decelerator Systems Technology Conference and Seminar, Monterey, CA, May 19-22, 2003.
- [11] Potvin J. and Peek G.; "PIMS Simulation Software Upgrade with a New Model for Slider-Reefed Parafoil Inflation. Comparison with Experimental Data"; March 25, 2007. Unpublished.
- [12] Baldwin, D. A., Kolb, L. M., Wittendorfer, K. E. and Nagel, L.; *Qualification tests for service use of the USMC MC-5 Ram Air Parachute Assembly (Free fall or static line configuration)*; China Lake report, NAWCWPNS TM 7330. Released on November 1992.

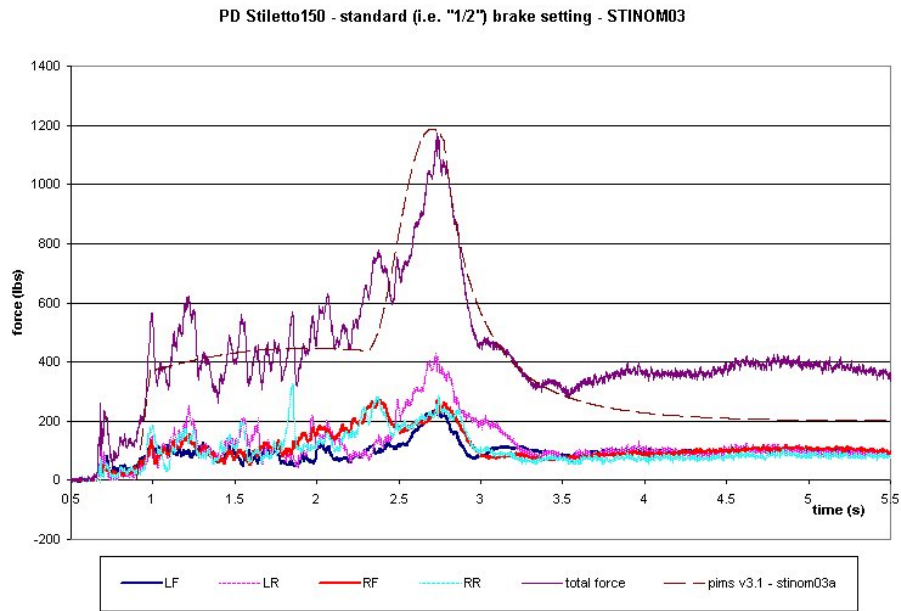
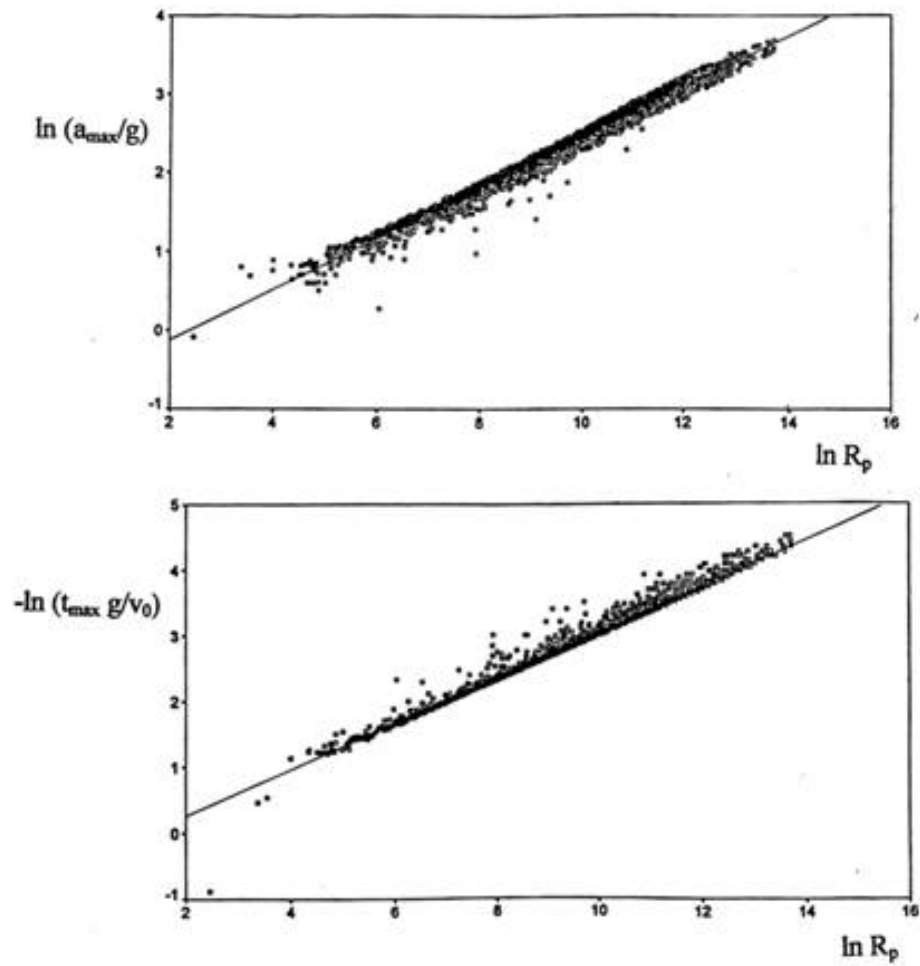


**Figure 1. Riser load evolution graph for a typical skydiving parafoil, namely a Performance Designs Stiletto 150 carrying a 200lbs payload. The jagged lines correspond to the actual load measured on each of the four risers. The dotted line corresponds to the 3-stage computer model discussed in reference [1].**



Maximum deceleration and time of maximum deceleration as obtained from numerical solution of the IPM over 2000 designs<sup>18</sup>; numerical data plotted against the dimensionless ratio  $R_p$  defined in Eq. (10) (data from Ref. 18).

Figure 2. Numerical data obtained from a large number of numerical simulations of the slider-descent model typified by equation (2) (graph extracted from reference [2]).

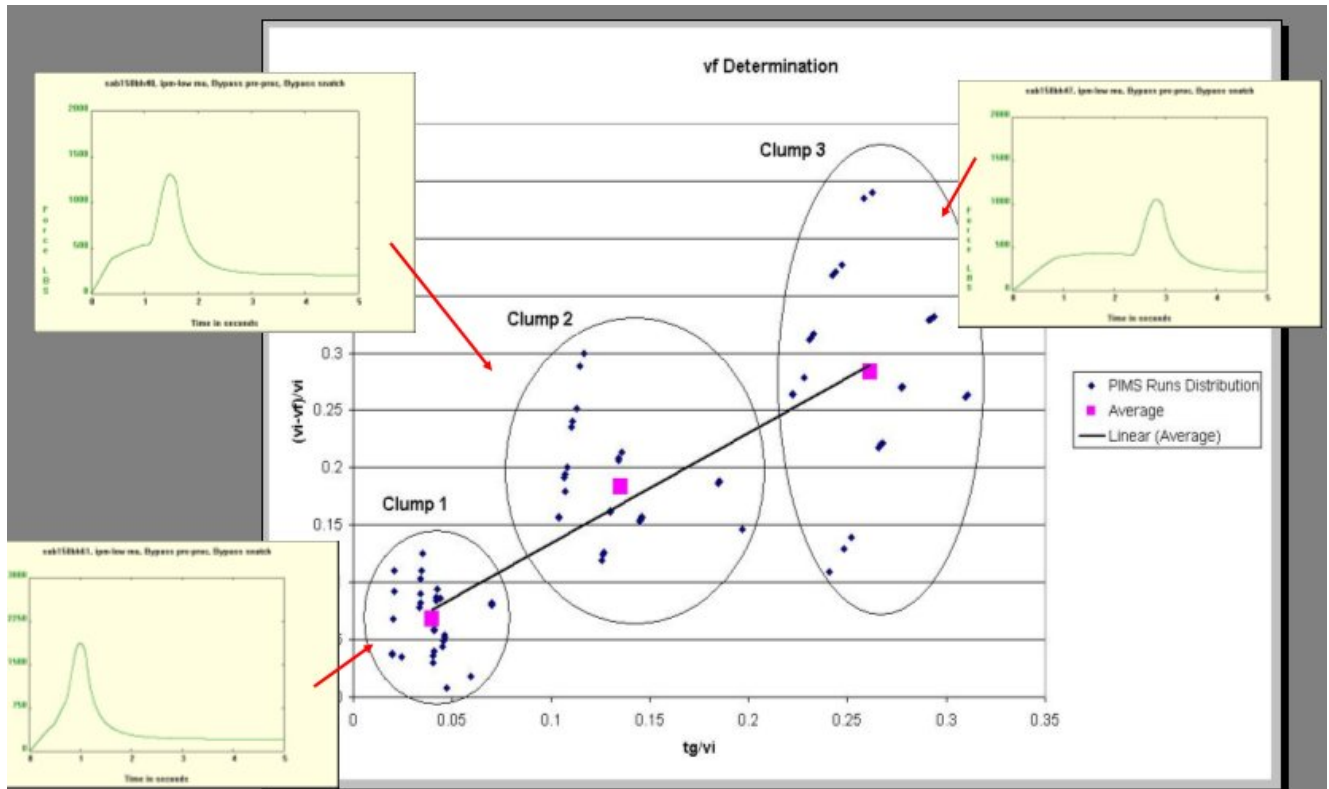


Figure 3. Computer simulations of the 3-stage inflation model of reference [1]: ratio  $(V_{stretch} - V_0)/V_{stretch}$  versus  $g\Delta t_{sliderup}/V_{stretch}$ . The sub-graphs show the parachute the type of drag evolutions that correspond to each “clump”.



Figure 4. Riser load evolution graph for a skydiving parafoil, namely a Performance Designs Sabre 230 carrying a 200lbs payload. This example highlights the rare constant- $SC_D$  slider-up inflation mode.

$$V_0 \approx V_{ff} = \sqrt{\frac{2W}{\rho(SC_D)_{nochute}}}$$

USMC MC-5/freefall/3611bs

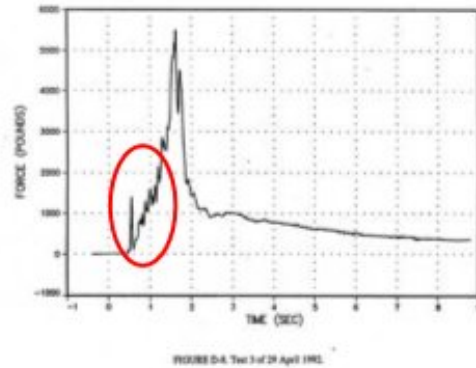


Figure 5. Typical riser load evolution graph of a USMC MC-5, seven-cell parafoil. Note the short slider-descent phase in this case. Illustration extracted from reference [12].